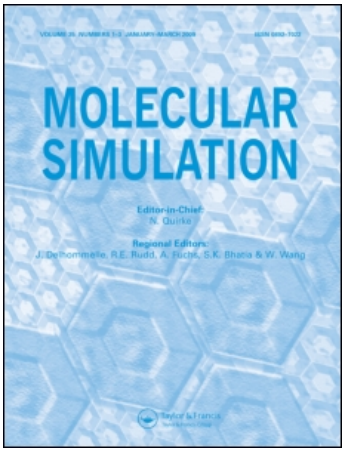

Molecular Simulation
Publication details, including instructions for authors and subscription information:
http://www.informaworld.com/smpp/title~content=t713644482

Monte Carlo Simulations of Primitive Model (PM) Electrolytes in Non-Euclidean Geometries

Shabnam Hanassab[a]; T. J. VanderNoot†[a]
[a] Chemistry Department, Queen Mary, University of London, London, United Kingdom

To cite this Article Hanassab, Shabnam and VanderNoot†, T. J.(2004) 'Monte Carlo Simulations of Primitive Model (PM) Electrolytes in Non-Euclidean Geometries', Molecular Simulation, 30: 5, 301 — 311
To link to this Article: DOI: 10.1080/08927020410001662624
URL: http://dx.doi.org/10.1080/08927020410001662624

Molecular Simulation, Vol. 30 (5), 30 April 2004, pp. 301–311

Taylor & Francis
Taylor & Francis Group

Monte Carlo Simulations of Primitive Model (PM) Electrolytes in Non-Euclidean Geometries

SHABNAM HANASSAB* and T.J. VANDERNOOT†

Chemistry Department, Queen Mary, University of London, Mile End Road, London E1 4NS, United Kingdom

(Received December 2003; In final form December 2003)

Monte Carlo canonical ensemble (*NVT*) simulations of unrestricted primitive model electrolytes (PM) on the 3D "surface" of a 4D hypersphere are reported here. The effects of concentration, ionic charge and/or ionic radii on the mean internal energy ($\langle U \rangle$), individual and mean ionic activities ($\langle \gamma_+ \rangle$, $\langle \gamma_- \rangle$ or $\langle \gamma_\pm \rangle$) and the mean net charge density distributions were studied. Our results showed that either higher charge, higher concentration or smaller ionic radii favoured ion–ion aggregation. The individual ionic activity coefficients of ions with different radii and/or charge differed significantly at higher concentrations. We also compared mean ionic activity coefficients for aqueous KCl and NaBr from simulations with reported experimental values in the literature and the agreement within 0.7–10%, depending upon concentration were found.

Keywords: Monte Carlo simulations; Primitive model (PM) electrolytes; Non-Euclidean; Spherical boundary conditions; Hyperspherical and individual ionic activity coefficient

INTRODUCTION

The simulation of electrolytes has been the focus of numerous studies over the past few decades [1–43]. The motivation for the long-standing interest in electrolyte models has been the need for more accurate simulation models, from which the thermodynamics and structural behaviour of electrolytes can be explained and predicted.

In order to perform reliable computer simulations of electrolytes it is of prime importance to consider interactions obeying the fundamental laws of electrostatics in the considered geometry. The Euclidean geometry with periodic boundary conditions (PBC) is the geometry which has been used most in Monte Carlo (MC) and Molecular Dynamics (MD) simulations of electrolytes [5–20,25–43]. Ewald summation has been used in simulations of electrolytes to account for the long-range contributions to the energy of ion–ion interactions. However, Ewald summation was originated for solving lattice-like systems and hence it is not as suitable for use in simulations of *disordered* electrolyte solutions. The main disadvantage with the Ewald method is that an electrolyte solution is not a true periodic lattice. The Ewald correlations do not decay with distance and the screening effect (which is a very important feature of electrolytes) is disregarded. Another problem with Ewald summation is that if the two particles lie along one of the principal axes of the periodic array of boxes and are separated by a distance which is half of the box length, then there is no effective force or interaction between the two particles which is unrealistic [47]. The Ewald summation is meant to include all the long-range interactions and that also makes it a computationally expensive method [4,52,55].

An elegant geometry which can be used in simulations of electrolytes is that of "spherical boundary conditions" (SBC), which is a non-Euclidean geometry. In SBC the particles are placed on the 2D surface of a 3D sphere or within the "3D" surface of a 4D hypersphere. The admirable feature of SBC is that it is a self-contained space and the number of particle–particle interactions is finite, because each pair of particles can only interact through the two geodesic curves (great circles), joining those two particles together and there is no

*Corresponding author. E-mail: s.hanassab@qmul.ac.uk
†E-mail: tjv@cognitrix.com

ISSN 0892-7022 print/ISSN 1029-0435 online © 2004 Taylor & Francis Ltd
DOI: 10.1080/08927020410001662624

need for particle images to be involved. Consequently, there is no need for any truncation or approximation in SBC geometry and this property makes SBC especially attractive in simulations of Coulombic systems. Furthermore, the previous results in simulations of electrolytes in SBC [2] indicated that the ion–ion interactions are considerably weaker through the longer geodesic and it is possible to neglect this contribution to the interactions without producing any statistically significant change in the final results. Therefore, this makes the simulations even more faster and efficient.

In a previous paper [2] canonical ensemble (*NVT*) MC simulations of RPM electrolytes in three dimensional (3D) non-Euclidean geometries (3D surface of a 4D hypersphere) were considered. The data from simulations in 3D Euclidean geometries reported in the literature were compared to the simulation results and they showed good agreement. A major advantage of non-Euclidean geometries is the system size independence of the structural and thermodynamic properties of the system [1]. Hence, for simulations of Coulombic systems the 3D non-Euclidean geometry is a very good alternative to the Euclidean geometry with PBC.

Caillol and co-workers used SBC in simulations of electrolytes [21–24,48–56]. In one case they reported that the computational time for a few hundred charged hard-spheres with dipolar hard-sphere solvent in 3D SBC was reduced by a factor of two or three compared to the same simulation performed in a Euclidean geometry with PBC and Ewald summation [55]. The aspects of Caillol's methods were discussed elsewhere [1].

Most of the groups who have studied electrolyte solutions by means of simulations have used the "restricted primitive model" (RPM) [1–36], which corresponds to hard-sphere cations and anions with equal radii and equal but opposite charges in a structureless dielectric continuum representing the solvent. The RPM is the most studied model of electrolyte systems and using this system, it is possible to compare the data obtained from any new approach with the existing literature.

However, in real electrolytes the cations and anions have unequal radii and often unequal charge magnitudes. As a result, the cations and anions will possess different individual ionic activity coefficients. Experimentally, it is not possible to measure individual ionic activity coefficients, but computer simulations can provide values for the individual ionic activity coefficients. Simulations of RPM electrolytes can provide only mean ionic activity coefficients, because the individual ionic activity coefficients for both the ions are the same. However, in the case of "primitive model" (PM) electrolytes where the hard-sphere cations and anions have different radii and/or charge magnitudes, the individual ionic activities will be different and the mean ionic activity coefficient will provide partial information at the best. The theoretical calculations of individual ionic activity coefficients at higher concentrations is beset by various assumptions, as in Debye-Hückel limiting law.

Very little work has been devoted to simulation of PM electrolytes [30–43]. In order to have a good simulation model, which would produce results comparable to experiments, the influence of the ionic radii must be investigated in detail. The simulations of the PM model can also be useful in studying the interface between two immiscible electrolyte solutions (i.e. oil and water interface), where the ions with different radii would have tendencies to be solvated in different phases. The computer simulations of this sort of inhomogeneous system will be reported in future publications [62].

Sloth and Sørensen [39] studied single ionic activity coefficients for 1:1 and 2:1 PM electrolytes using the HyperNetted Chain (HNC) approximation. They found that single ionic activity coefficients were largely unaffected by the relative size of the ions at low concentrations (corresponding to large interionic separations). However, the ionic charges were shown to significantly affect the single ionic activities. They also studied a case in which the radii of cations and anions were different at a fixed Bjerrum parameter and higher concentrations [40]. They found that the single ionic activity coefficients of the ions with different radii were significantly different from one another.

Abramo *et al.* [42] have reported MC simulations for 1:1 and 2:2 electrolytes with unequal radii for the cations and anions. Their results showed that as the cation to anion radius ratio ($r_+/r_- = \alpha$) decreased, the electrostatic energy became more negative. At smaller α, the maximum of the peak in the pcf between like ions was enhanced, compared to an electrolytic system of $\alpha = 1$. Basically, as the smaller ion in the system decreased in size, ion–ion clustering was favoured and there were longer electrostatic interactions.

There are two main computational methods from which individual ionic activity coefficients can be calculated: particle insertion [44] or particle deletion [45]. Since these two methods are biased under certain conditions, it is more reasonable and accurate to use some combination of them. The hybrid method was first proposed by Kumar [46] who used it successfully in simulations of Lennard–Jones systems. An alternative hybrid method was proposed by VanderNoot and Panayi [4] for simulations of Coulombic systems because Kumar's formula did not produce reasonable answers in simulations of electrolytes. The method of VanderNoot and Panayi was used in simulations of RPM electrolytes and the observed results were in good agreement with

the values of activity coefficients reported in the simulation literature at lower concentrations. The discrepancies between hybrid method results and the simulation literature at higher concentrations were studied by VanderNoot [3]. VanderNoot [3] concluded that in the simulation literature, cases of hard sphere overlap were included in the other calculations, leading to artefacts in the calculations of activity coefficients.

In the literature, reduced variables have often been used because many possible combinations of actual or real variables will correspond to the same state and the calculations performed on one combination can give equivalent results for other combinations [22–31, 37–40]. In this way, unnecessary simulations are avoided. For the RPM simulations, the appropriate dimensionless reduced variables are the Bjerrum parameter (B^*) and reduced density (ρ^*). In the case of PM electrolytes previous workers [30–43] have used an additional reduced variable which is the radius ratio of the cation to anion r_+/r_-). However, we have found in simulations of the PM electrolytes, where both the charge magnitudes and radii of the ions are different, the charge ratio (q_+/q_-) must also be considered as an additional reduced variable. This is because, in the cases where the charge ratios differ but the charge products are identical, the Bjerrum parameter, B^*, fails to account for this. Any two systems with the same charge product (i.e. B^* value), but different charge ratios (e.g. 3:1 or $\sqrt{3}$:$\sqrt{3}$) possess very different thermodynamic properties. In simulations of the PM model where the charges and the radii of the cation and anion are unequal, four different reduced variables are required. In this work, we decided not to use (four) reduced variables since it only requires six variables to specify simulation conditions in a format consistent with experimental measurements. For our work the computational time difference for using four or six variables was marginal. Also, when comparing our results to the experimental values, the additional effort of converting reduced variables to actual variables was avoided.

All the groups who have studied PM electrolytes by simulations have used Euclidean geometries [30–43]. In this paper we report the use of a 3D non-Euclidean geometry in simulations of PM electrolytes consisting of ions with asymmetric charges and/or unequal radii over a range of concentrations. We also simulated aqueous KCl and NaBr and compared the corresponding mean ionic activity coefficients with the reported experimental values.

COMPUTATIONAL METHOD

The 3D hyperspherical MC simulation program which was used in the previous work was used in this work as well (all details are given elsewhere) [1–3]. We carried out simulations of 1:1 and 2:2 electrolytes with variable radii using SBC geometry over a range of concentrations at room temperature. In addition, we carried out simulations for systems with charges of 1:1, 1:2, 1:3, 2:1, 2:2, 2:3, 3:1, 3:2 and 3:3 (the first charge corresponds to the cation and the second that of the anion) over a range of concentrations from 0.0001 M up to 0.1 M.

In studying the effects of charge on the behaviour of the asymmetric electrolytes, the radii of the anion and the cation were considered to be unequal. In order to be more realistic, the average hydrodynamic radii of some typical cations and anions in each charge group were calculated from the molar conductivities of those particular ions reported in the literature using the formula [57]:

$$r_i = \frac{z^2F^2}{6\pi N_A \lambda_i^o \eta} \tag{1}$$

where r_i is the hydrodynamic radius of an ion (i.e. the radius of the ion including the hydration shell), z is the integral charge of the ion, F is the Faraday, N_A is Avogadro's constant, λ_i^o is the molar conductivity of the ion and η is the viscosity of the solvent. Notice that in this way the mean hydrodynamic radii used for each particular charge in our simulations represent an average over typical values for ions of that charge. The mean value was taken and used as a typical anionic or cationic radius in the simulations of electrolytes with asymmetric charges. The mean hydrodynamic radii which were used in this work are presented in Table I.

In all simulations a system size of $N = 100$ was used, except for electrolytes with charge ratios of 1:2 or 2:1 in which the system size was $N = 102$ (divisible by 3), in order to produce an electroneutral system. The temperature and solvent permittivity were set as 300 K and 78.4 (for bulk water), respectively.

Finally we compared our calculated values of mean ionic activity coefficient to the reported experimental literature values by running some simulations with identical conditions to the measurements of some real electrolytes. In this case, we used the same approach as before (Eq. 1)

TABLE I Average hydrodynamic radius for each particular charge to represent an average over typical values for ions of that charge

z	*Average hydrodynamic radius/pm*
+1	200
+2	650
+3	1200
− 1	140
− 2	500
− 3	900

TABLE II The calculated hydrodynamic radii of the cation and anion for two different electrolytes: aqueous KCl and NaBr. The Pauling radii for these ions are also shown in this table

Ion	*Hydrodynamic radius/pm*	*Pauling radius/pm*
K^+	125.3	133.0
Na^+	183.8	97.0
Cl^-	120.6	181.0
Br^-	117.9	196.0

to calculate the hydrodynamic radii of the cation and anion for two different electrolytes: aqueous KCl and NaBr. The hydrodynamic radii used for these compounds are shown in Table II. We also used the Pauling radii (Table II) in our simulations as well as a radius of 250 pm (as used in previous work [1–3]) to compare with the experimental values. The main reason that we selected these compounds to test our model was that the cation and anion in each compound have similar radii and they are also symmetric in charge. By keeping the situation as simple as possible, we minimised the likelihood of unexpected deviations caused by charge and radii which were dramatically different. Anions and cations with similar radii and charges are more likely to experience similar interactions with the solvent.

RESULTS AND DISCUSSION

Asymmetric Ionic Radii

Four sets of simulations at four different concentrations: 0.001, 0.01, 0.1 and 1.0 M were run for 1:1 and 2:2 electrolytes for a range of ionic radii from 100 to 400 pm. All other conditions were kept constant throughout the simulations ($T = 300$ K, $\varepsilon = 78.4$ and $N = 100$). The simulation time for the electrolytes consisting of ions with larger radii or higher concentrations were longer, as expected, due to the higher volume fraction within the simulation cell or larger electrostatic interactions. In these cases the acceptance ratio for successful particle insertion was also lower, due to hard-sphere overlap of the particles (hard-sphere overlap was not allowed) or less favourable energy change.

Figure 1(a) and (b) represent the 3D plots of reduced mean internal energy versus ionic radii of cation and anion for 1:1 and 2:1 electrolytes, respectively. The results indicated that the internal energy decreased as the size of the ions decreased or the concentration of the solution increased. By decreasing the radii and/or increasing the concentration, the ion–ion separations decreased and the electrostatic interactions were stronger, so the mean internal energy decreased as a consequence.

The corresponding graphs of mean individual ionic activities ($\langle\gamma_+\rangle$ and $\langle\gamma_-\rangle$) against ionic radii are presented in Fig. 2(a), (b). These show that the activity coefficients of the individual ions in the system decreased as the ions became smaller, the charge increased or the concentration increased. Interestingly, the graphs show that the individual ionic activity coefficient of one type of ion depended upon the ionic radius of the oppositely charged ion. As the ionic radius of the oppositely charged ion increased the individual ionic activity coefficient of the other ion became more positive. The strength of interactions will be affected by the interionic distance of closest approach (or contact) between the two ions. This effect was stronger and more noticeable at higher concentrations.

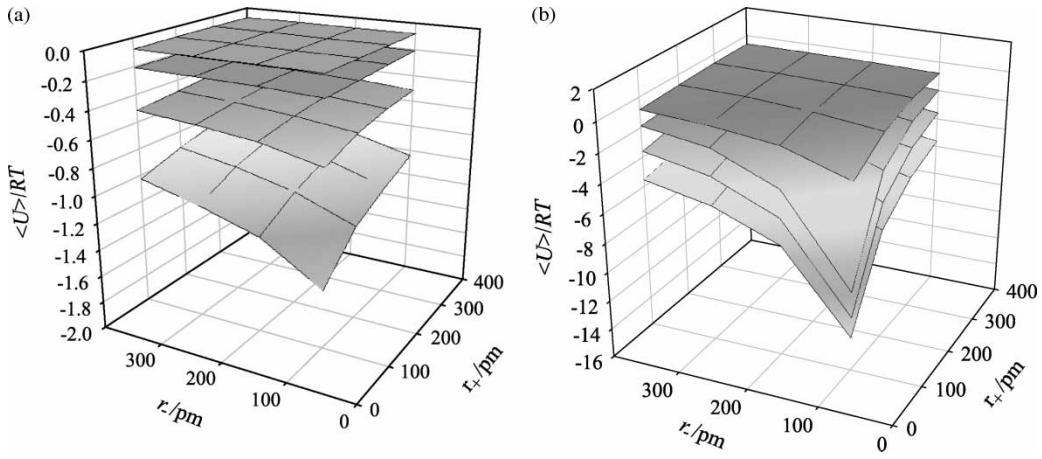

FIGURE 1 A 3D graph showing the reduced mean internal energy, $\langle U\rangle/RT$, versus the ionic radii of the anions and cations at four different concentrations. The topmost surface corresponds to the lowest concentration (0.001 M) and the lowest layer is from the highest concentration of 1.00 M. The other two layers in between are for the 0.01 and 0.1 M solutions. The conditions for the simulations were: $\varepsilon = 78.4$, $N = 100$ and $T = 300$ K, (a) 1:1 electrolytes and (b) 2:2 electrolytic solution.

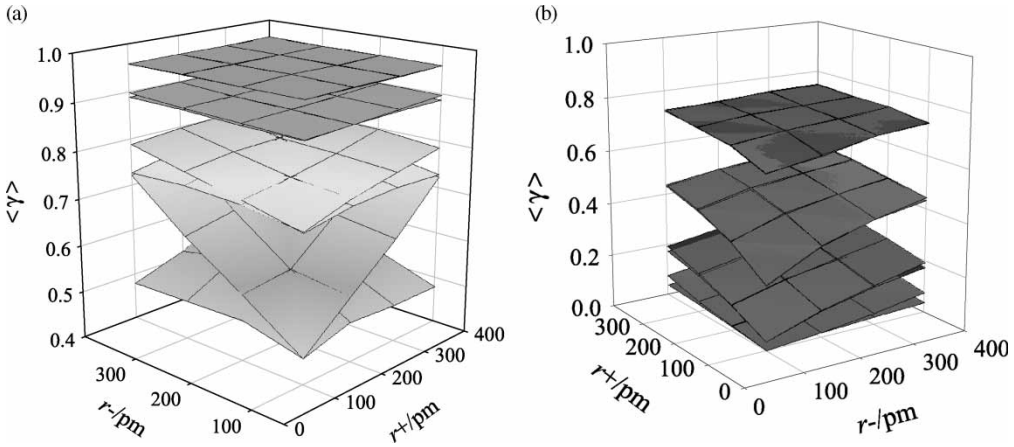

FIGURE 2 A 3D graph showing the mean individual ionic activity coefficients $\langle\gamma_+\rangle$ and $\langle\gamma_-\rangle$, versus the ionic radii of the anions and cations at four different concentrations. The lowest concentration is the top layer and the bottom layer indicates the most concentrated solution. However, each layer consist of two individual surfaces or "sheets" for $\langle\gamma_+\rangle$ and $\langle\gamma_-\rangle$. At lower concentrations there is a complete overlap of these two, but at higher concentrations they appear as distinct. The conditions for the simulations were: $\varepsilon = 78.4$, $N = 100$ and $T = 300\,\mathrm{K}$, (a) 1:1 electrolytes and (b) 2:2 electrolytic solution.

The position of the ions in the system was studied, and thus demonstrated that as the radii of the ions became smaller, the ions started to form aggregates or clusters. This was because the electrostatic forces at short range between two small oppositely charged ions were stronger than those between two larger ions. Therefore, with higher electrostatic interactions, the ions tended to associate and the energy of the system (and hence the ionic activities) decreases (Fig. 3(a),(b)).

Asymmetric Charges

A series of simulations were run with varying charge products corresponding to electrolytes from 1:1 to 3:3 (cation : anion), in the concentration

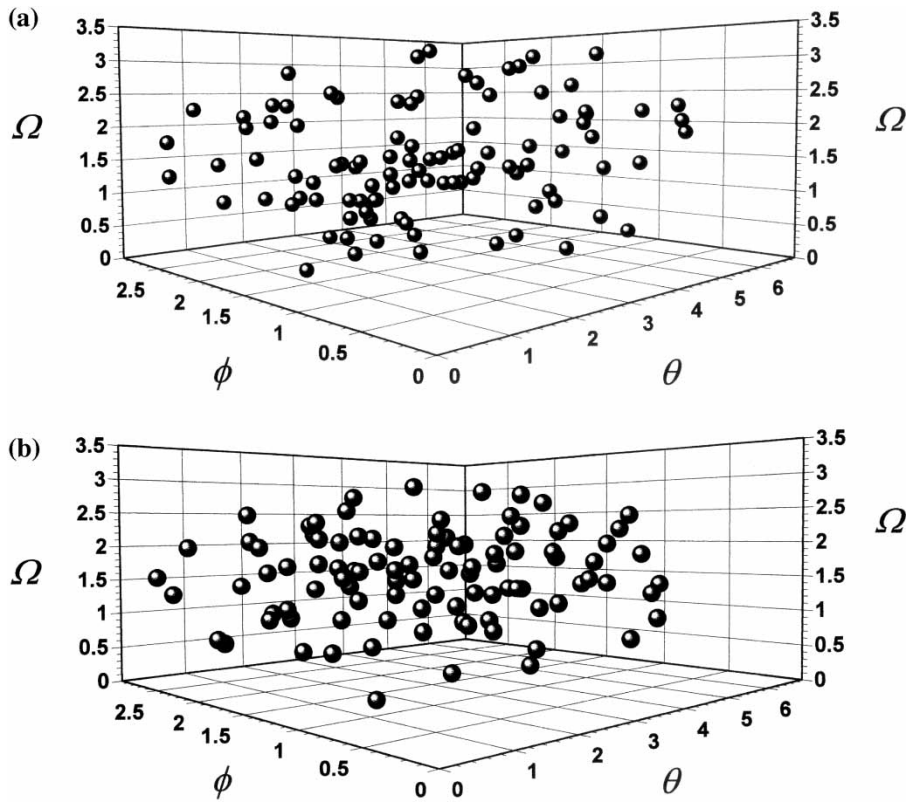

FIGURE 3 A 3D graph showing the positions of the ions in the simulation cell. The three axes on the graph indicate the spherical angles (in radians) θ, Φ and Ω. The simulation conditions were $T = 300\,\mathrm{K}$, $c = 1.00\,\mathrm{M}$, $\varepsilon = 78.4$, $q_i = \pm 2$, and $N = 100$, (a) $r_+ = r_- = 100\,\mathrm{pm}$ and (b) $r_+ = r_- = 400$. Notice the larger amount of empty space in (a), where there is higher ion–ion aggregations.

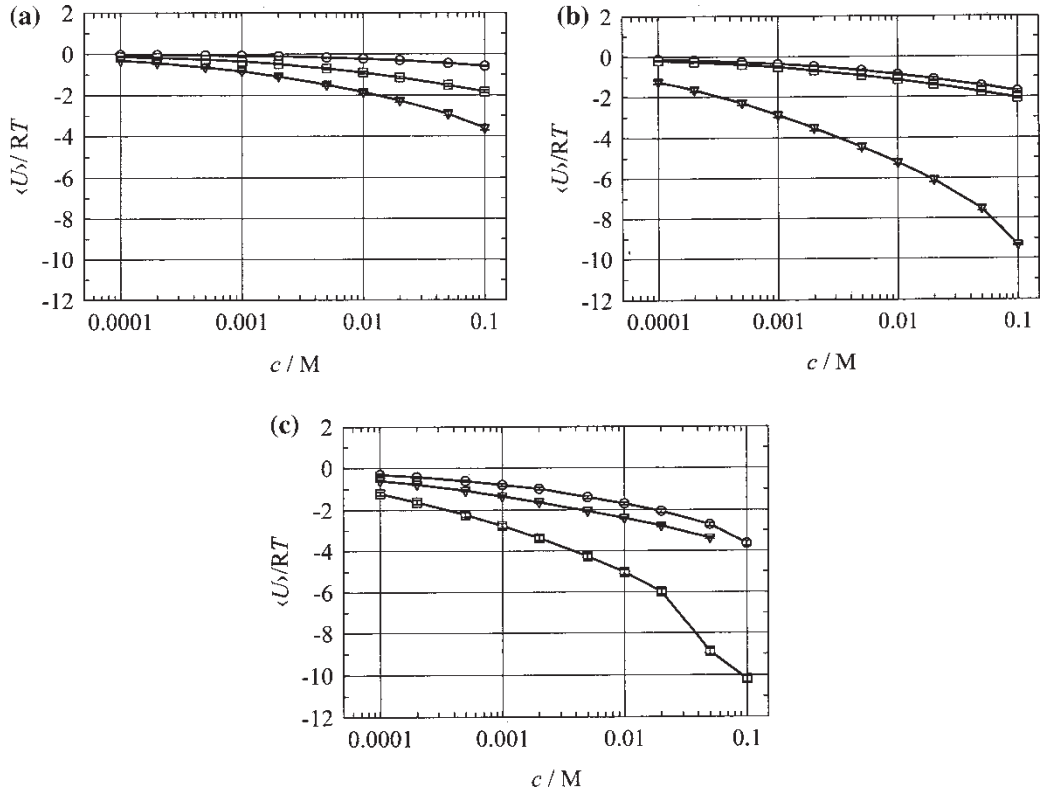

FIGURE 4 Reduced mean internal energy, $\langle U\rangle/RT$, as a function of concentration (M). The conditions of the simulations were: $T = 300\,\mathrm{K}$, $\varepsilon = 78.4$ $r_{\pm} = 250\,\mathrm{pm}$ and $N = 100$ or 102 (as indicated in the text). A single standard deviation is indicated in our data by the error bars. (a) (o—o) for 1:1, (□—□) for 1:2 and (▽—▽) for 1:3 electrolytes (b) (o—o) for 2:1, (□—□) for 2:2 and (▽—▽) for 2:3 electrolytes (c) (o—o) for 3:1, (□—□) for 3:2 and (▽—▽) for 3:3 electrolytes.

range 0.0001–0.5 M and having the other simulation conditions constant ($T = 300\,\mathrm{K}$, $\varepsilon = 78.4$, $N = 100$ or $N = 102$ for 1:2 and 2:1 electrolytes in order to maintain electroneutrality of the system). In some cases (e.g. charge 3:3) the ions had large radii and their successful insertion into the system during the moves was less likely because of frequent hard-sphere overlap. So for these cases, 0.05 M was the highest concentration studied conveniently.

The reduced mean internal energies as a function of concentration for different charge ratios are shown in Fig. 4(a)–(c). The results show that the reduced mean internal energy decreased with increasing concentration. The electrolytes with charges of 2:3 and 3:2 had lower internal energies than the other combinations and this effect was more pronounced at higher concentrations.

From studying the net charge density distributions of 2:1 and 2:3 electrolytes (Fig. 5(a), (b)), we observed

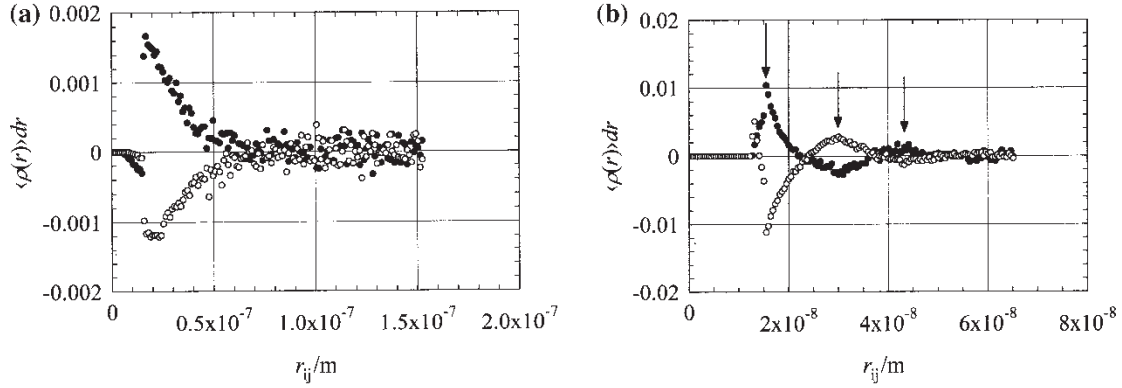

FIGURE. 5 A graph of the mean net charge density, $\langle\rho(r)\rangle$, within a spherical shell of thickness dr, as a function of radial distance from the central ion. The full circles correspond to the distribution of positive ions around a negative central ion and the hollow circles correspond to the distribution of negative ions around a positive central ion for (a) 2:1 and (b) 2:3 electrolytes. The simulation conditions were: $T = 300\,\mathrm{K}$, $\varepsilon = 78.4$, $c = 0.05\,\mathrm{M}$ and $N = 100$ or 102 and the ionic radii as shown in Table I. Note that the single peak in 5(a) indicate the formation of ion pairs whereas the three peaks in 5(b) indicate the formation of ion quadruplets.

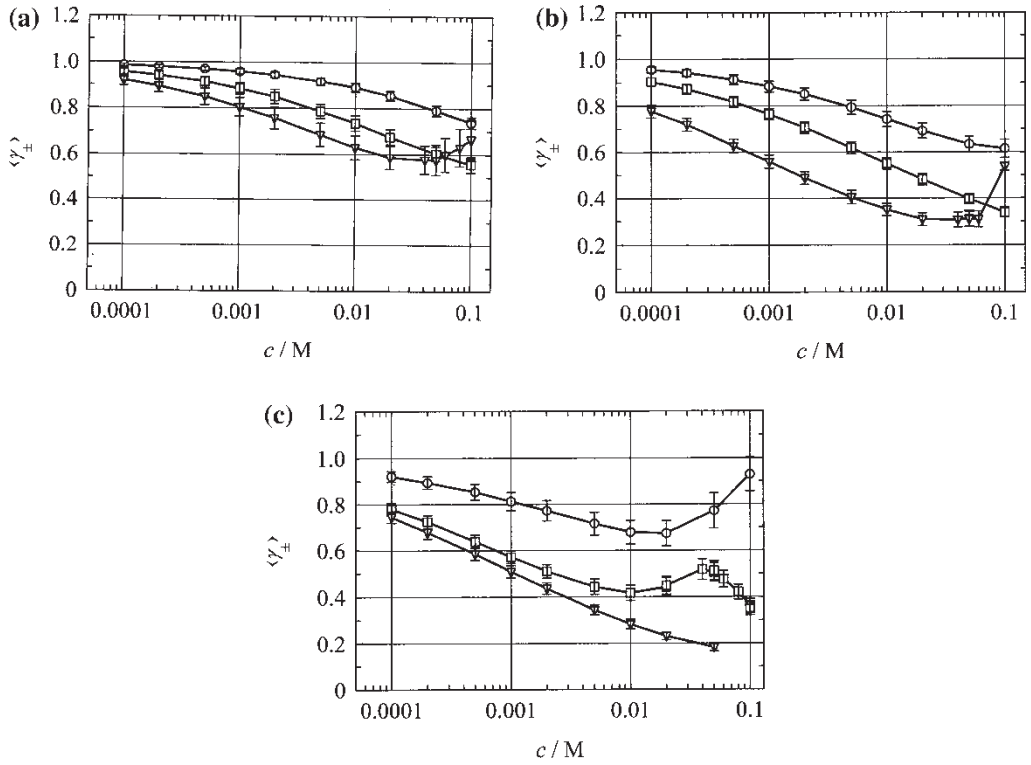

FIGURE 6 Mean ionic activity coefficient $\langle r_\pm \rangle$ as a function of concentration (M). The conditions of the simulations were: $T = 300\,\mathrm{K}$, $\varepsilon = 78.4$, $r_\pm = 250\,\mathrm{pm}$ and $N = 100$ or 102 (as indicate in the text). A single standard deviation is indicated on our data by the error bars. (a) (o—o) for 1:1, (□—□) for 1:2 and (▽—▽) for 1:3 electrolytes (b) (o—o) for 2:1, (□—□) for 2:2 and (▽—▽) for 2:3 electrolytes (c) (o—o) for 3:1; (□—□) for 3:2 and (▽—▽) for 3:3 electrolytes.

distributions which were different for these two charge combinations. On both graphs, the region where the net charge density was near zero corresponded to the hard-sphere exclusion region. For the 2:1 electrolyte (Fig. 5(a)), the first peak in the distribution was due to the presence of the first nearest ion to the central ion. Beyond the first peak, there is random noise about the average value of zero corresponding to a random arrangement of ions with respect to the central ion. Therefore, for the 2:1 electrolytes the single peak in the distribution means that the ions were aggregating in solution to form principally ion pairs. For the 2:3 electrolyte (Fig. 5(b)) we can see three distinct peaks in the distribution, indicating that there were three ions associated in close proximity with the central ion. This means that the ions were aggregating to form clusters as large as quadruplets. Hence, the formation of larger aggregates (quadruplets versus pairs) was the reason why the highly charged asymmetric electrolytes (2:3 and 3:2) had dramatically lower internal energies than the other electrolyte combinations studied here.

Figure 6(a)–(c) shows the mean ionic activity versus concentration for different charge ratios. The mean ionic activities decreased as the charge product and/or concentration increased. However, there were exceptions for 1:3, 2:3, 3:1 and 3:2, where an upward curvature was noticed at concentrations above 0.03 M. From studying the individual ionic activity coefficients for anions and cations of these systems, it was observed that with increasing concentration, the value of $\langle\gamma_+\rangle$ increased again (became more positive) while $\langle\gamma_-\rangle$ decreased continuously (more negative). Consequently, the mean ionic activity of these two individual activities would show an overall upward curvature (Fig. 7(a), (b)). This shows that the activities of individual ions can differ dramatically depending upon their charge and size. The difference between the activities of the cations and anions can be understood in terms of the difference in interactions of the cations and anions. As noted previously [4], associating ions tend to form "chains". Chains of ions maximise the attractive interactions and minimise the repulsive interactions. So for a 2:3 electrolyte, a chain would consist of three $+2$ cations and two -3 anions (Fig. 8). If the electrostatic energy of interactions (total of attractive and repulsive interactions) within this chain is calculated for the cations and anions (with hydrodynamic radii, Table II), then the mean electrostatic energy for each cation is $-1.2002 \times 10^{-20}\,\mathrm{J}$ and for each anion it is $-1.8477 \times 10^{-20}\,\mathrm{J}$. This shows that the cations have weaker interactions than the anions and hence higher ionic activities than the anions which experience stronger

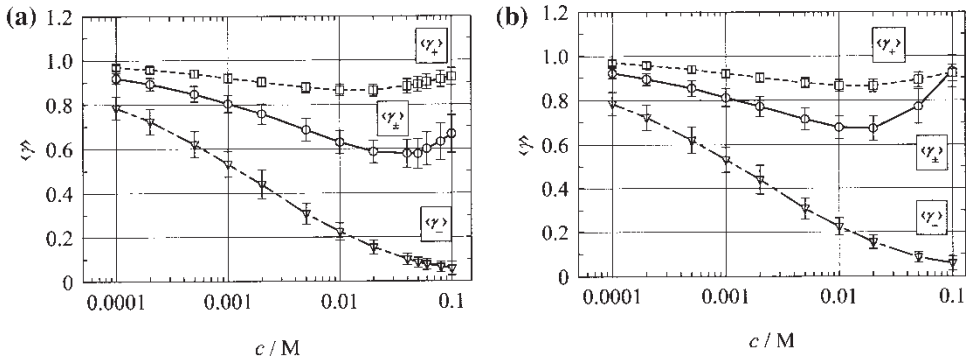

FIGURE 7 Mean ionic activity coefficient $\langle\gamma_{\pm}\rangle$ (o—o), single cationic activity coefficient $\langle\gamma_{+}\rangle$ (□—□) and single anionic activity coefficient $\langle\gamma_{-}\rangle$ (▽—▽) as functions of concentration (M). The conditions of the simulations were: $T = 300\,\mathrm{K}$, $\varepsilon = 78.4$ and $N = 100$ or 102 (as indicated in the text). The value of the ionic radii is also given Table I. A single standard deviation is indicated on our data by the error bars. (a) 1:3 electrolyte (b) 2:3 electrolyte.

interactions in a chain. The difference in electrostatic energies is responsible for the differing ionic activities of the cations and anions.

Simulations versus Experiments

In 1976, Larsen [11] showed that the simulated thermodynamic properties of the simulated RPM in PBC were in good qualitative agreement with certain real salt properties although some qualitative discrepancies suggested that a real salt could not be fully understood in terms of RPM.

The groups who have studied the RPM model by means of simulations have used ionic radii in the range of 215–250 pm [4,8,17,21,25,43]. Fundamentally, the ionic radius was considered higher than the Pauling ionic radii, in order to account for the solvation shell around the cations and anions.

A useful simulation model should produce results which are in agreement with the macroscopic system. The PM would be expected to give results which are more comparable to the experimental data. However, choosing the correct ionic radii when the solvent is modelled as a dielectric continuum is an issue. In real solutions a shell of solvent molecules forms around the ions, and this increases the effective size of the ions beyond the bare radii (Pauling radii) [58]. Llano-Restrepo and Chapman [34] simulated aqueous alkali halides solutions, using the Pauling radii as the ionic hard-sphere radii and setting the hard-core radius of the water molecules to the mean value of the cation and anion Pauling radii. They compared their results of the hydration numbers with the reported experimental data and found a reasonable agreement.

Sloth and Sørensen [39] used HNC to predict the activity coefficient for aqueous KCl solutions (as a PM electrolyte) where the solvent was represented by "water-like" polarizable polar hard-spheres. They used the ionic radii of K = 151 pm and Cl = 162 pm and found a good agreement from their HNC approximation to the experimental data for aqueous KCl solutions.

In this part of the work, we explored the accuracy of our PM simulations by running some simulations under conditions similar to real experiments, and then compared our results for the ionic activities with literature values at 298 K [59]. In order to do this, we chose aqueous solutions which consisted of cations and anions with similar ionic radii, to keep the situation as simple as possible and for which the experimental mean ionic activity coefficients were available in the literature.

We simulated Coulombic systems consisting of KCl or NaBr over a range of concentrations and compared the mean ionic activity coefficients with the literature values. We tried three variations of ionic radii for each of KCl and NaBr. In the first case we used the hydrodynamic radii (Table II) calculated from Eq. (1). In the second case we used the Pauling radii (Table II) and finally a radius of 250 pm was used as in previous works [1–4].

It is important to consider the fact that in the literature [59] concentrations were presented in molality, whereas our simulations were based on the concentration units of molarity. As a result a unit conversion of molality into molarity was done [60] and the simulation was run at the corresponding calculated molarity value. However, we have shown

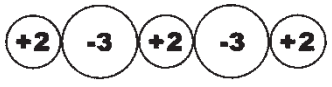

FIGURE 8 An electroneutral chain of ions for a 2:3 electrolyte. The radii of the ions are shown with the same proposition as their hydrodynamic radii. Note that a chain will maximise attractive interactions and minimise repulsive interactions.

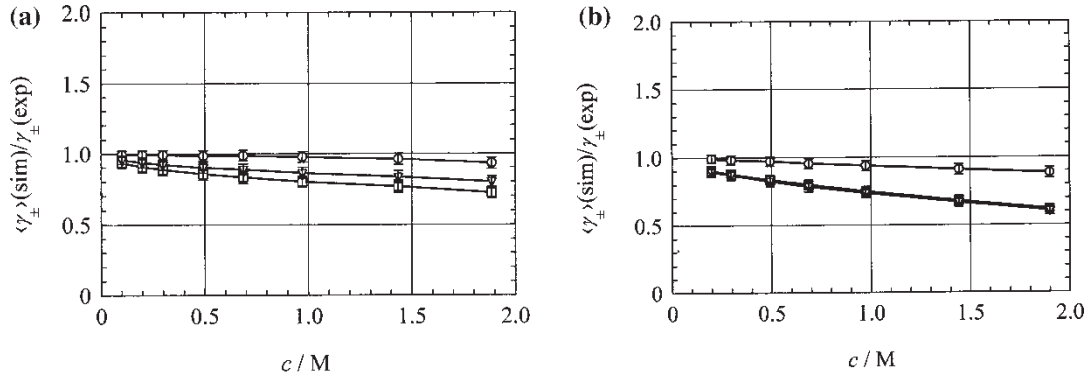

FIGURE 9 The ratio of mean ionic activity coefficient $\langle\gamma_\pm\rangle$ from the PM simulations to the experimental value of the corresponding system versus concentration (M) (a) KCl (b) NaBr. The simulation conditions were: $\varepsilon = 78.4$, $N = 100$, $T = 300$ K. The three curves show the results from different radii: $\langle r_\pm\rangle = 250$ pm (o—o); hydrodynamic radii (□—□) and Pauling radii (▽—▽), from Table II.

our results in terms of molarity, since this has been used in previous work.

Figure 9(a), (b) shows the ratios of mean ionic activity coefficient from the simulations to that of the experiments versus concentration for KCl and NaBr, respectively. The best agreement from the simulations to the experimental data was observed where the ionic radii of 250 pm for cations and anions for solutions was used. The variation of simulations to experiments was from 0.7% (0.1 mol kg^{-1}) up to 7% (2.00 mol kg^{-1}) for KCl and from 0.9% (0.2 mol kg^{-1}) up to 12% (2.00 mol kg^{-1}) for NaBr. The comparison of our results with the experimental values (using hydrodynamic radii or Pauling radii) are shown in Tables III and IV.

Our results agreed well with the experimental values at lower concentrations. The discrepancies between simulations and experimental results became larger at higher concentrations. We believe that the discrepancies between simulation and experimental values at higher concentrations could be due to several possible causes:

(i) in real electrolytes, as the ions get closer to one another, their hydration shells may overlap together allowing the ions to get closer than expected on the basis of hydrodynamic radii (Fig. 10(a)–(c)). In the simulations, the particles were hard spheres and they could not overlap. Additionally, the radii were constant at all concentrations. It has been suggested by Larsen [11] that replacement of the hard-cores by soft repulsive potentials will shift the properties of the simulated electrolytes towards the corresponding experimental results. We will report our results for the simulations of soft-core electrolytes in future [61].

(ii) the solvent is only a dielectric continuum (structureless solvent) in our simulations, whereas in the real experiments the solvent consists of individual dipolar particles. Therefore, there are no interactions of individual solvent molecules with the ions and any effect from solvent fluctuations or discreteness is excluded. In an electrolyte solution solvent molecules in close proximity to an ion orient themselves and polarization takes place. Consequently, in that region the solvent premittivity is lower than the bulk and the ions will have a lower ionic activity than expected. The issue of solvent molecule orientation and polarizability is completely ignored in RPM and PM models, as the solvent is assumed to be a dielectric continuum.

TABLE III A table to show the percentage variation of the mean ionic activity coefficients calculated from simulations to the reported experimental values as various ionic radii were used for the simulations of KCl

	Radius value/pm		
c/mol kg^{-1}	*250*	*Hydrodynamic*	*Pauling*
0.1	0.7%	6.8%	1.2%
2.0	7.0%	28%	10%

TABLE IV A table to show the percentage variation of the mean ionic activity coefficients calculated from simulations to the reported experimental values as various ionic radii were used for the simulations of NaBr

	Radius value/pm		
c/mol kg^{-1}	*250*	*Hydrodynamic*	*Pauling*
0.2	0.9%	9.7%	1.8%
2.0	12.0%	38.3%	26.6%

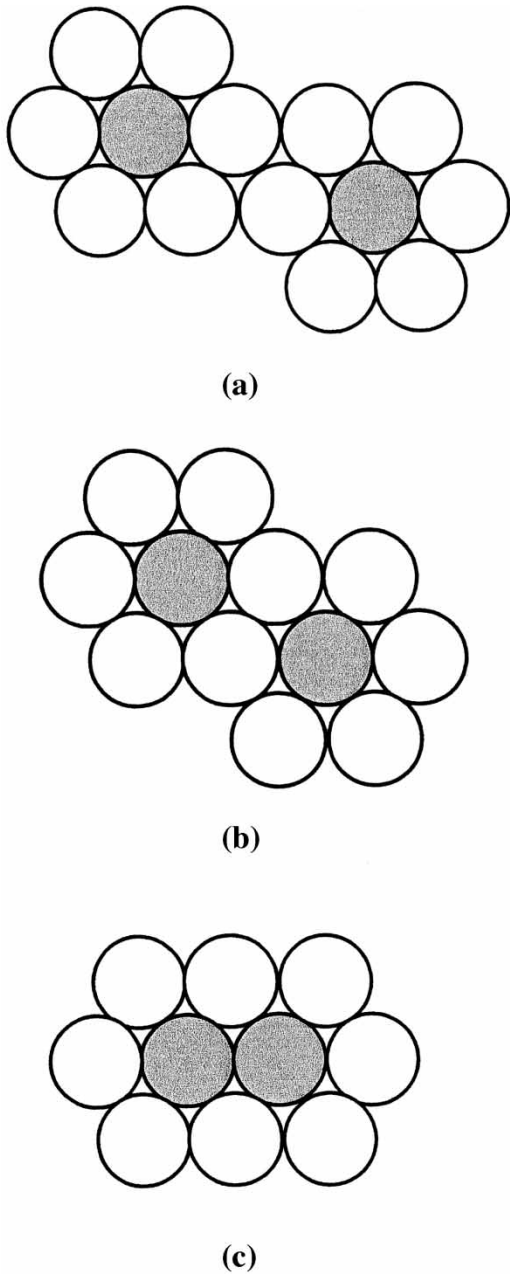

FIGURE 10 A diagram showing the progressive overlap of the hydration shells in a real electrolyte, the darker circle indicates the bare ion and the lighter circles represent solvent molecules around the ion (a) solvation shells are intact (b) solvation shells overlap (c) ion–ion contact pair within a solvent cage.

CONCLUSIONS

(1) Non-Euclidean geometries are a suitable and reliable geometry to use in simulations of electrolytes. Results from our simulations show surprising agreement to experimental results, especially considering the simplicity of the PM simulation model.
(2) The individual ionic activity coefficient of one ion depends upon the ionic radius of the opposite charged ion.
(3) The individual ionic activity coefficients for cations and anions with asymmetric charge and/or radii are drastically different from one another within a system.

References

[1] Hanassab, S. and VanderNoot, T.J. (2003) "Spherical boundary conditions: a finit and system size independent geometry for simulations of electrolytic liquids", *Mol. Simul.* **29**, 527.
[2] Hanassab, S. and VanderNoot, T.J. (2002) "Monte Carlo simulations of restricted primitive model (RPM) in non-Euclidean geometries", *J. Electroanal. Chem.* **528**, 135.
[3] VanderNoot, T.J. (2000) "Factors affecting the calculations of mean ionic activities in Monte Carlo simulations of primitive model electrolytes", *PCCP* **2**, 253.
[4] VanderNoot, T.J. and Panayi, A. (1998) "Monto Carlo simulations of restricted primitive electrolytes in a 2D non-Euclidean geometry", *J. Chem. Soc., Faraday Trans.* **94**, 1939.
[5] Card, D.N. and Valleau, J.P. (1970) "Monte Carlo study of the thermodynamic of electrolyte solutions", *J. Chem. Phys.* **52**, 6232.
[6] Hummer, G. and Soumpasis, D.M. (1993) "The correlations and free energies in restricted primitive model descriptions of electrolytes", *J. Chem. Phys.* **98**, 581.
[7] Valleau, J.P., Cohen, L.K. and Card, D.N. (1980) "Primitive model electrolytes. II. The symmetrical electrolyte", *J. Chem. Phys.* **72**, 5942.
[8] Vlachy, V., Ichiye, T. and Haymet, A.D.J. (1991) "Symmetric associating electrolytes: GCMC simulations and integral equation theory", *J. Am. Chem. Soc.* **113**, 1077.
[9] Rasaiah, J.C., Card, D.N. and Valleau, J.P. (1972) "Calculations on the resticted primitive model for 1:1 electrolyte solutions", *J. Chem. Phys.* **56**, 248.
[10] Lyubartsev, A.P., Martinovski, A.A. and Shevkunov, S.V. (1992) "New approach to Monte Carlo calculation of the free energy: method of expanded ensemble", *J. Chem. Phys.* **96**, 1776.
[11] Larsen, B. (1976) "Studies in statistical mechanics of Coulombic systems I. Equation of state for the restricted primitive model", *J. Chem. Phys.* **65**, 3431.
[12] Bresme, F., Lomba, E., Weis, J.J. and Abascal, J.L.F. (1995) "Monte Carlo simulation and integral-equation studies of a fluid of charged hard spheres near the critical region", *Phys. Rev. E.* **51**, 289.
[13] Bresme, F. and Abascal, J.L.F. (1993) "Pair connectedness functions and percolation in highly charged electrolyte solutions", *J. Chem. Phys.* **99**, 9037.
[14] Van Megan, W. and Snook, I.K. (1980) "The grand canonical ensemble Monte Carlo method applied to electrolyte solutions", *Mol. Phys.* **39**, 1043.
[15] Torrie, G.M. and Valleau, J.P. (1980) "Electrical double layers I. Monte Carlo study of a uniformly charged surface", *J. Chem. Phys.* **73**, 5807.
[16] Sloth, P. (1992) "Electrochemical potentials in the grand canonical ensemble: some formal and numerical results for confined ionic systems", *Mol. Phys.* **77**, 667.
[17] Valleau, J.P. and Card, D.N. (1972) "Monte Carlo estimation of the free energy by multistage sampling", *J. Chem. Phys.* **57**, 5457.
[18] Rogde, S.A. and Hafskjold, B. (1983) "Equilibrium properties of a 2:2 electrolyte model, Monte Carlo and integral equation results for the restricted primitive model", *Mol. Phys.* **48**, 1241.
[19] Sloth, P., Sørensen, T.S. and Jensen, J.B. (1987) "Monte Carlo calculations of thermodynamic properties of the restricted, primitive model of electrolytes at extreme dilution using 32, 44, 64, 100, 216 and 512 ions and *ca.* 10^6 configurations per simulation", *J. Chem. Soc., Faraday Trans.* 2 **83**, 881.
[20] Sørensen, T.S. (1991) "Error in the Debye-Hückel approximation for dilute primitive model electrolytes with Bjerrum

parameters of 2 and *ca.* 6.8 investigated by Monte Carlo methods", *J. Chem. Soc., Faraday Trans.* **87**, 479.
[21] Caillol, J.M. (1993) "A new potential for the numerical simulations of electrolyte solutions on a hypersphere", *J. Chem. Phys.* **99**, 8953.
[22] Caillol, J.M. and Weis, J.J. (1995) "Free energy and cluster structure in the coexistence region of the restricted primitive model", *J. Chem. Phys.* **102**, 7610.
[23] Caillol, J.M. (1994) "A Monte Carlo study of the liquid–vapour coexistence of charged hard spheres", *J. Chem. Phys.* **100**, 2161.
[24] Weis, J.J., Levesque, D. and Caillol, J.M. (1998) "Restricted primitive model of an ionic solution confined to a plane", *J. Chem. Phys.* **109**, 7486.
[25] Sloth, P. and Sørensen, T.S. (1988) "Monte Carlo simulations of single-ion chemical potentials: preliminary results for the restricted primitive model", *Chem. Phys. Lett.* **143**, 140.
[26] Sevensson, B.R. and Woodward, C.E. (1988) "Widom's method for uniform and non-uniform electrolyte solutions", *Mol. Phys.* **64**, 247.
[27] Karaska, T. (1997) "Widom's method for uniform and non-uniform electrolyte solutions", *Mol. Phys.* **90**, 165.
[28] Vega, C., Bresme, F. and Abascal, J.L.F. (1996) "Fluid–solid equilibrium of a charged hard-sphere model", *Phys. Rev. E* **54**, 2746.
[29] Pitzer, K.S. and Schreiber, D.R. (1987) "The restricted primitive model for ionic fluids, properties of the vapour and the critical region", *Mol. Phys.* **60**, 1067.
[30] Sørensen, T.S. (1993) "Direct calculation of the electric potential distributions around ions from high precision canonical ensemble Monte Carlo simulations of some primitive model electrolyte systems", *Mol. Simul.* **11**, 267.
[31] Sørensen, S. (1990) "How wrong is the Debye-Hückle approximation for dilute primitive model electrolytes with moderate Bjerrum parameter", *J. Chem. Soc., Faraday Trans.* **86**, 1815.
[32] Valleau, J.P. and Cohen, L.K. (1980) "Primitive model electrolytes. I. Grand canonical Monte Carlo computations", *J. Chem. Phys.* **72**, 5935.
[33] Sevensson, B.R. and Woodward, C.E. (1988) "Widom's method for uniform and non-uniform electrolyte solutions", *Mol. Phys.* **64**, 247.
[34] Liano-Restrepo, M. and Chapman, W.G. (1994) "Monte Carlo simulation of the structural properties of concentrated aqueous alkali halide solutions at 25°C using a simple civilized model", *J. Chem. Phys.* **100**, 8321.
[35] Rogde, S.A. (1983) "Monte Carlo results for an electrolyte-solution model. Divalent charged hard-spheres of unequal diameter", *Chem. Phys. Lett.* **103**, 133.
[36] Sevensson, B., Akesson, T. and Woodward, C.E. (1991) "On the simulation of thermodynamic and structural properties of simple liquids", *J. Chem. Phys.* **95**, 2717.
[37] Sloth, P. (1992) "Electrochemical potentials in the grand canonical ensemble: some formal and numerical results for confined ionic systems", *Mol. Phys.* **77**, 667.
[38] Sloth, P. and Sørensen, T.S. (1990) "Monte Carlo calculations of chemical potentials in ionic fluids by application of Widom's formula: correction for finite-system effects", *Chem. Phys. Lett.* **173**, 51.
[39] Sloth, P. and Sørensen, T.S. (1990) "Single-ion activity coefficients and structure of ionic fluids. Results for the primitive model of electrolyte solutions", *J. Chem. Phys.* **94**, 2116.
[40] Sloth, P. and Sørensen, T.S. (1988) "Monte Carlo simulations of single ion chemical potentials: results for the unrestricted primitive model", *Chem. Phys. Lett.* **146**, 452.
[41] Rasaiah, J.C. (1972) "Computations for higher valence electrolytes in the restricted primitive model", *J. Chem. Phys.* **56**, 3071.
[42] Abramo, M.C., Caccamo, C., Malescio, G., Pizzimenti, G. and Rogde, S.A. (1984) "Equilibrium properties of charged hard spheres of different diameters in the electrolyte solution regime: Monte Carlo and integral equation results", *J. Chem. Phys.* **80**, 4396.
[43] Corti, H.R., Laria, D. and Trevani, L.N. (1996) "Ionic association in asymmetric electrolytes", *J. Chem. Soc., Faraday Trans.* **92**, 91.
[44] Widom, B. (1963) "Some topics in the theory of fluids", *J. Chem. Phys.* **39**, 2808.
[45] Shing, K.S. and Gubbins, K.E. (1982) "The chemical potential in dense fluids and fluid mixtures via computer simulations", *Mol. Phys.* **46**, 1109.
[46] Kumar, S.K. (1992) "A modified real particle method for the calculations of the chemical potentials of molecular systems", *J. Chem. Phys.* **97**, 3550.
[47] Valleau, J.P. and Whittington, S.G. (1977) "A guide to Monte Carlo for statistical mechanics: 1. Highways. In Statistical Mechanics. A", *A Modern Theoretical Chemistry* (B.J. Berne, New York), pp 137–168.
[48] Hansen, J.P., Levesque, D. and Weis, J.J. (1979) "Self-diffusion in the two-dimensional, classic electron gas", *Phys. Rev. Lett.* **43**, 979.
[49] Kratky, K.W. (1980) "New boundary conditions for computer experiments of thermodynamic systems", *J. Comp. Phys.* **37**, 205.
[50] Kratky, K.W. and Schreiner, W. (1982) "Computational techniques for spherical boundary conditions", *J. Comp. Phys.* **47**, 313.
[51] Caillol, J.M. and Levesque, D. (1991) "Numerical simulations of homogeneous and inhomogeneous ionic systems: an efficient alternative to the Ewald method", *J. Chem. Phys.* **94**, 597.
[52] Caillol, J.M. and Levesque, D. (1992) "Structural, thermodynamic and electrical properties of polar fluids and ionic-solutions on a hypersphere: results of simulations", *J. Chem. Phys.* **96**, 1477.
[53] Caillol, J.M. (1993) "Search of the gas–liquid transition of dipolar hard spheres", *J. Chem. Phys.* **98**, 9835.
[54] Caillol, J.M. (1992) "Structural, thermodynamic and electrical properties of polar fluids and ionic solutions on a hypersphere: theoretical aspects", *J. Chem. Phys.* **96**, 1455.
[55] Delville, A., Pellang, R.J-M. and Caillol, J.M. (1997) "A Monte Carlo (*NVT*) study of the stability of charged interfaces: a simulation on a hypersphere", *J. Chem. Phys.* **106**, 7275.
[56] Caillol, J.M. (1999) "Numerical simulations of Coulomb systems: a comparison between hyperspherical and periodic boundary conditions", *J. Chem. Phys.* **111**, 6528.
[57] Hibbert, D.B. (1993) *Introduction to Electrochemistry*, 1st Ed. (Macmillan Publishers, UK), p 113.
[58] Weast, R.C. (1974–1975) *Handbook of Chemistry and Physics*, 55th Ed. (CRC Press) p. F-198.
[59] Conway, S. (1952) *Electrochemical Data Book* (Elsevier Publishing Company), pp 86–87.
[60] Weast, R.C. (1974–1975) *Handbook of Chemistry and Physics*, 55th Ed. (CRC Press), p D-119.
[61] Hanassab, S. and VanderNoot, T.J (2003) "Monte Carlo simulations of soft-sphere electrolytes in non-Euclidean geometries", in preparation.
[62] Hanassab, S. and VanderNoot, T.J (2003) "Computer simulations of the Interface between Two Immiscible Electrolyte Solutions (ITIES) in spherical boundary conditions", In preparation.